The Bound States of Amphipathic Drugs in Lipid Bilayers: Study of Curcumin

Yen Sun,* Chang-Chun Lee,* Wei-Chin Hung,† Fang-Yu Chen,‡ Ming-Tao Lee,§ and Huey W. Huang*
*Department of Physics and Astronomy, Rice University, Houston, Texas 77251; †Department of Physics, Chinese Military Academy, Fengshan, Kaohsiung 83055, Taiwan; ‡Department of Physics, National Central University, Chung-Li 32054, Taiwan; and §National Synchrotron Radiation Research Center, Hsinchu, 30076 Taiwan

ABSTRACT Drug-membrane interactions are well known but poorly understood. Here we describe dual measurements of membrane thickness change and membrane area change due to the binding of the amphipathic drug curcumin. The combined results allowed us to analyze the binding states of a drug to lipid bilayers, one on the water-membrane interface and another in the hydrocarbon region of the bilayer. The transition between the two states is strongly affected by the elastic energy of membrane thinning (or, equivalently, area stretching) caused by interfacial binding. The data are well described by a two-state model including this elastic energy. The binding of curcumin follows a common pattern of amphipathic peptides binding to membranes, suggesting that the binding states of curcumin are typical for amphipathic drugs.

INTRODUCTION

The lipid matrix, or the lipid bilayer, of cell membranes is a natural binding site for amphipathic molecules, including proteins, organic molecules such as drugs, detergents, and others. However the biological effect of drug-membrane interactions (1) is unclear. For example, if drugs must diffuse through membranes to bind to specific protein targets, then binding to the membrane may cause a secondary effect distinct from that of the drug-protein interaction. Whether the membrane-binding produces desirable or undesirable effects, it is important to understand the effect of drug binding to lipid bilayers, since there are concrete examples that a change of the physical state of the lipid bilayer can affect the functions of embedded proteins (2,3). It is well recognized that amphipathic molecules can bind to the membrane-water interface or intercalate into the nonpolar chain region (1). As far as we know, the energetics of these two binding states of drugs and their effects on lipid bilayers have not been analyzed. In this work we show that the dual measurements of both the membrane thickness and the membrane area changes due to drug binding allow such analyses.

Curcumin is an example of amphipathic drugs that bind to cell membranes (4,5). This yellow spice has long been reported to be biologically active, most often as having anti-inflammatory, antiangiogenic, antioxidant, wound-healing, and anticancer effects (6,7). However its efficacy has been a subject of controversy (8), and its mechanism of action remains obscure. In particular, curcumin modulates the function and expression of a wide range of structurally and functionally unrelated membrane proteins, which suggests that curcumin might alter membrane protein function by modulating the properties of the host lipid bilayer (2). In a recent work, we reported a nonlinear thinning effect on lipid bilayers caused by curcumin binding (9). This was found by an x-ray diffraction measurement of the bilayer thickness as a function of curcumin content. The thinning result allowed us to explain the effect of curcumin on the lifetime of the gramicidin single channel (2,9). To gain a more complete understanding of the curcumin-membrane interactions, we report here a systematic measurement of the responses of individual giant unilamellar vesicles (GUVs) to the binding of curcumin from solution. The GUV experiment measured the change of the membrane area due to curcumin binding, to be compared with the corresponding membrane thinning. From these two results, we are able to deduce the binding states of curcumin in lipid bilayers. We construct a simple two-state model assuming that there are two distinct bound states for curcumin—one at the interface and another in the hydrocarbon chain region. The energy of the interfacial binding state includes the elastic energy of the membrane thinning. This simple model reproduces the experimental data.

The choice of the two experimental methods was in part motivated by the desire to answer these questions: Is an effect on membranes measured in a multilamellar preparation, as used in x-ray diffraction experiments, reproducible by a measurement of a single membrane in solution, as in a GUV experiment? Are the two measurements quantitatively compatible? These questions are affirmatively answered by the agreement between the membrane-thinning measured in multilamellae and the membrane area increase measured in GUVs. The quantitative analysis of these two sets of data provides an example for applying similar analyses to other membrane-binding molecules.

We found that the binding behavior of curcumin follows the same pattern as more hydrophilic amphipathic peptides.

Submitted March 17, 2008, and accepted for publication April 30, 2008.

Address reprint request to Dr. Huey W. Huang, Dept. of Physics and Astronomy, Rice University, Houston, TX 77251-1892. Tel.: 713-348-4899; Fax: 713-348-4150; E-mail: hwhuang@rice.edu.

Editor: Paul H. Axelsen.

0006-3495/08/09/2318/07 $2.00

doi: 10.1529/biophysj.108.133736

This implies that the binding states of curcumin are typical of amphipathic drugs.

MATERIALS AND METHODS

Materials

1,2-dioleoyl-*sn*-glycero-3-phosphocholine (DOPC) and 1,2-dioleoyl-*sn*-glycero-3-phosphoethanolamine-*N*-(lissamine rhodamine B sulfonyl) (Rh-DOPE) were purchased from Avanti Polar Lipids (Alabaster, AL). 3,3′-dioctadecyloxacarbocyanine perchlorate (DiO) was from Invitrogen (Carlsbad, CA). Curcumin (product number 28260), HEPES (product number H3375), bovine serum albumin (BSA) (product number A9418), and dimethyl sulfoxide (DMSO) were from Sigma-Aldrich (St. Louis, MO). All materials were used as delivered.

Sample preparation

Curcumin (Fig. 1 *a*) can be dissolved in water by first dissolving it in DMSO. But the water solubility and the molecular stability of curcumin is strongly pH dependent. The aqueous solubility decreases as pH decreases below 7, but the molecule degrades as pH increases above 7 (10). Therefore a buffer solution of 20 mM HEPES was used to maintain the solution at pH 7. Optical spectroscopy was employed to calibrate the curcumin concentration and to monitor its molecular integrity (10). In our previous study (9), we showed that at pH 7 the solubility limit for curcumin is ~25 μM. Curcumin was first dissolved in DMSO at 19 mM and then diluted with sucrose/HEPES solution to desired concentrations (<25 μM). Almost all previous GUV studies by the aspiration method were performed in 100–200 mM sucrose solutions (11,12). The curcumin solutions were kept in the dark as much as possible because curcumin is sensitive to light (13). Also, curcumin adsorbed to the walls of containers, often 5%–20%, depending on the material and the surface/volume ratio of the container. The loss of curcumin to the container wall at each step of solution transfer was carefully monitored by a spectral measurement (9). We also took into account the fraction of curcumin adhered to the wall of the experimental chamber. We estimated the uncertainty of the curcumin concentration in the experimental chamber to be approximately ±10%.

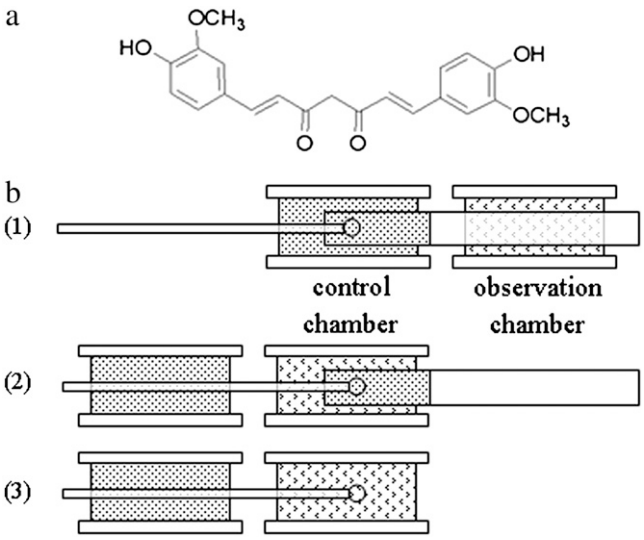

FIGURE 1 (*a*) Chemical structure of curcumin. (*b*) Schematic of the GUV experiment (see text). (*1*) An aspirated GUV was inserted ~0.7 mm into the transfer pipette in the control chamber. (*2*) The aspirated GUV in the transfer pipette was moved from the control chamber to the observation chamber. (*3*) Then the transfer pipette was swiftly moved away so that the GUV was exposed to the curcumin/sucrose/HEPES solution (marked as $t = 0$).

GUV experiment

GUVs were produced in 200 mM sucrose solution by the electroformation method (14). DOPC and a 0.4% molar ratio of a headgroup fluorescent lipid were codissolved in chloroform. A fluorescent lipid was added to enhance the contrast of the GUV boundary. We found no difference between the two fluorescent lipids Rh-DOPE and DiO. The lipid solution was dried onto two platinum electrodes. After drying under vacuum, the electrodes were placed 5 mm apart in a chamber filled with 200 mM sucrose solution. We applied 1.5 V alternating current at a frequency of 10 Hz across the electrodes for 10 min. Then the voltage was changed to 3 V, and the frequency was adjusted to 10 Hz for 40 min, followed by 3 Hz for 15 min, 1 Hz for 10 min, and 0.5 Hz for 30 min. This electroformation method has been shown to produce unilamellar large vesicles (14). The vesicle suspension was then gently collected in a glass vial. The vesicles were used within 24 h of production.

To perform the GUV experiment, the vesicles were first transferred to a control chamber containing an ~180 mM sucrose and 20 mM HEPES solution. The osmolality of every solution used in the GUV experiment was measured by a Wescor Model 5520 dew point Osmometer (Wescor, Logan, UT). The osmolality of the solution in the control chamber was the same as the 200 mM sucrose solution inside the GUVs. A micropipette (of inner radius 8–10 μm) was used to hold a chosen GUV (of 25–35 μm in radius) by aspiration at a constant negative pressure (which created a membrane tension of 0.5 dyn/cm (15)). Before use, the micropipette was coated with 0.5% BSA to neutralize the charge on the bare glass surface (16) and washed extensively by 200 mM sucrose solution. The tail end of the aspiration pipette was connected to a pressure control system constructed similarly to a setup described by Fygenson et al. (17). A syringe was used to create a negative pressure inside the micropipette, which was referenced to the atmospheric pressure by a water-filled U tube. The value of the negative pressure was monitored via a manometer MKS Baratron 223 (Andover, MA) and recorded for postexperimental inspection. The curcumin experiment was performed by transferring the aspirated GUV to an observation chamber that contained a curcumin/sucrose/HEPES solution (see schematic in Fig. 1 *b*). The observation chamber was set side-by-side with the control chamber, separated by ~1 cm. A transfer pipette (inner diameter 0.75 mm) filled with the control solution was inserted from the opposite side of the aspiration pipette through the observation chamber into the control chamber. The aspiration pipette and the transfer pipette were held separately by motor-driven micromanipulators Narishige MM-188NE (East Meadow, NY). The aspirated GUV was inserted ~0.7 mm into the transfer pipette in the control chamber. By moving the microscope stage, the aspirated GUV in the transfer pipette was moved from the control chamber to the observation chamber. Then the transfer pipette was swiftly moved away so that the GUV was exposed to the curcumin/sucrose/HEPES solution (marked as $t = 0$).

If the observation chamber contained a sucrose/HEPES (without curcumin) solution isotonic to a 200 mM sucrose solution, the GUV remained unchanged, as expected. When curcumin was present in the solution of the observation chamber, the vesicle projection in the micropipette immediately increased its length and reached an equilibrium length within ~100 s. Thereafter the projection length remained unchanged. The video image of the process was captured by a Nikon NS-5 MC camera (Nikon, Tokyo, Japan) (Fig. 2). The response of GUVs indicated that the outer and inner leaflets of the bilayers changed their areas together, implying that the same amount of curcumin bound to both leaflets; otherwise there would be an areal imbalance between the outer and inner leaflets that was not observed. On a number of runs, we used glucose instead of sucrose in the observation chamber to measure the phase contrast between the inside and outside of the GUV and detected no change in the contrast during the entire process. This implied that there was no content exchange between the inside and outside of the GUV. We assumed that there was no change in the vesicle volume during curcumin binding. Then the increase of the vesicle projection in the micropipette can be

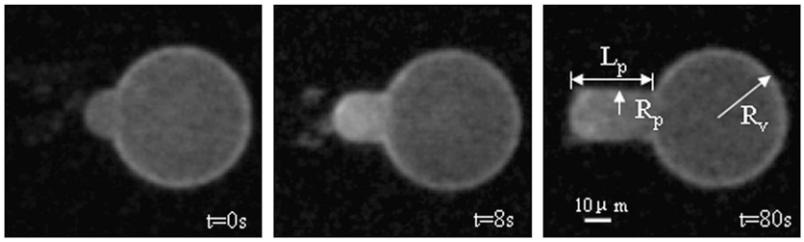

FIGURE 2 Sequential videomicrographs of a GUV held under a small constant pressure exposed to 8.96 μM curcumin solution. L_p, R_p, and R_v are indicated.

translated to an increase in the membrane area by the geometric relation (15) $\Delta A = 2\pi R_p(1 - R_p/R_v)\Delta L_p$, where R_p and R_v are radii of the pipette and vesicle, and L_p is the projection length (Fig. 2). All the values of R_p, R_v, and L_p were carefully measured and analyzed by using the Nikon NIS-Elements BR 2.30 software. To normalize the area changes for vesicles of different sizes, ΔL_p was converted to the fractional change of vesicle area $\Delta A/A$ plotted as a function of time (see below). To minimize the osmolality change due to evaporation, solutions in the chambers were changed frequently (approximately every 15 min).

Effect of DMSO

DMSO was used to solubilize curcumin in an aqueous solution of pH 7. The amount of DMSO used was proportional to the curcumin concentration. The highest curcumin concentration in our experiment was 13.5 μM (after the calibration for the losses to the container walls mentioned above), and its corresponding DMSO content was 0.16% (or 20 mM). DMSO has been shown to have no effect on lipid bilayer properties at such low concentrations. Longo et al. (11) showed that in the presence of 0.5% DMSO, the rupture tensions for lipid vesicles were the same as without DMSO. Hwang et al. (18) showed that DMSO at 0.8% did not affect the single channel lifetime of gramicidin. However, we found that DMSO presented a problem for the osmotic balance in a GUV experiment. For example when we used a solution of sucrose/HEPES and 0.16% DMSO in the observation chamber that was measured to have the same osmolality as the 200 mM sucrose solution inside the GUV, we found the vesicle projection length diminished and the GUV burst, indicating a tonicity imbalance. Apparently the GUV swelled, since, at constant vesicle surface area, the vesicle volume change ΔV is related to the projection length change by $\Delta V = -\pi R_p(R_v - R_p)\Delta L_p$. The most reasonable explanation is that the lipid bilayer is permeable to DMSO; therefore, DMSO did not contribute to the tonicity (the effective osmolality with respect to the membrane). This made the osmotic pressure outside the GUV lower than inside, hence causing swelling. However, if we added 0.16% DMSO to a sucrose/HEPES solution which was already isotonic to 200 mM sucrose solution inside the GUV and used it in the observation chamber, the vesicle projection length would increase slightly, indicating an outflow of water from the GUV. Apparently DMSO contributed slightly to the tonicity, not entirely consistent with DMSO being a permeant solute. This was also observed by Longo et al. (11).

Curcumin experiment

Since the interaction between DMSO and curcumin might alter the tonicity contribution by DMSO, we were not confident that the effect of DMSO is correctable by a background subtraction (11). Therefore, we performed the curcumin experiment in two ways to measure the upper and lower limits of the curcumin effect on the lipid bilayer. In the first experiment, the observation chamber contained a sucrose/HEPES/curcumin/DMSO solution of various curcumin concentrations. Each solution was measured to have the same osmolality as the 200 mM sucrose solution. The GUV response was recorded and plotted as $\Delta A/A$ vs. time in Fig. 3. In this case, the vesicle volume would somewhat increase and make the ΔL_p somewhat smaller than the pure curcumin effect. Therefore the measurement represented a lower limit of the curcumin effect.

In the second experiment, the observation chamber contained a sucrose/HEPES solution that was measured to have the same osmolality as 200 mM sucrose solution. Then the appropriate amount of curcumin/DMSO was added to obtain the desired curcumin concentration. The GUV response was recorded and plotted as $\Delta A/A$ versus time in Fig. 3. In this case, the vesicle volume would somewhat decrease and make the ΔL_p somewhat longer than the pure curcumin effect. Therefore the measurement represented an upper limit of the curcumin effect.

DISCUSSION

A lipid bilayer responds to molecular binding by changing its thickness and its surface area. If an amphipathic molecule binds to the water-membrane interface, it necessarily inserts between lipid headgroups and causes an interfacial area expansion. An interfacial area expansion will cause membrane thinning, due to the very small volume compressibility of hydrocarbon chains (19). The relation between the thickness

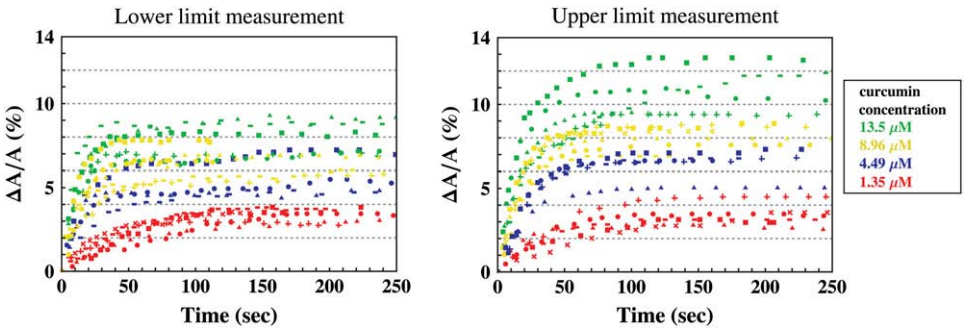

FIGURE 3 Time sequence of fractional area changes of individual DOPC GUVs exposed to various concentrations of curcumin: 13.5 μM (*green*), 8.96 μM (*yellow*), 4.49 μM (*blue*), 1.35 μM (*red*). Different symbols represent different runs. (*Left*) For each run, the osmolality of the solution in the observation chamber, including curcumin/DMSO, was made the same as the 200 mM sucrose solution inside the GUV. (*Right*) For each run, the curcumin/DMSO solution was added to a sucrose/HEPES solution that had the same osmolality as the 200 mM sucrose solution inside the GUV.

change and the area change due to an interfacial molecular binding is simply $-\Delta h/h = \Delta A/A$, where h is the thickness of the hydrocarbon region and A is the surface area of the lipid bilayer. On the other hand, if a molecule intercalates into the hydrocarbon chain region, it would certainly expand the membrane area, but it might not affect the membrane thickness.

Membrane thinning

The thickness of a phospholipid bilayer can be measured by its phosphate-to-phosphate distance (*PtP*) across the bilayer. The *PtP* of DOPC bilayers was previously measured by x-ray diffraction as a function of its curcumin content (9) and is reproduced in Fig. 4. The data show that the initial binding of curcumin has a large thinning effect up to the bound curcumin/lipid ratio of ~0.032, but the effect becomes considerably smaller upon further binding. Qualitatively, this indicates that there is one low-energy binding state that causes thinning and a higher energy binding state that has little thinning effect.

We consider the low energy state first. To the first few amphipathic molecules approaching a lipid bilayer, the interface, rather than the nonpolar chain region, is expected to be the lowest energy binding site. This has been proven for amphipathic peptides (mostly antimicrobial peptides (20)), which in all cases initially bind to the interface of lipid bilayers (21–24) by hydrophobic interactions (25). We will call this interfacial binding the *S* state and denote the area expansion per molecule by A_S. We know that to a very good approximation, the thickness of the hydrocarbon region is $h \approx PtP - 10$ Å, or *PtP* minus twice the length of the glycerol region (from the phosphate to the first methylene of the hydrocarbon chains) for pure lipid bilayers as well as for bilayers containing bound molecules (9). Let C_b be the total number of curcumin molecules bound to a bilayer of L lipid molecules. If the number of curcumin molecules in the *S* state is $N(S)$, then we have the membrane thinning due to the curcumin molecules bound to the S state:

$$-\Delta h/h = \Delta A/A = A_S N(S)/A_L L, \tag{1}$$

where A_L is the cross section area for each lipid molecule in the bilayer.

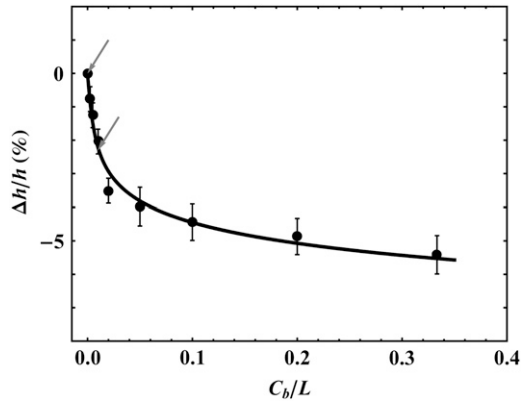

FIGURE 4 Fractional thickness change of DOPC bilayer as a function of curcumin content, expressed as bound curcumin/lipid molar ratio C_b/L. The data are from Hung et al. (9). Two arrows indicate the points that were used to determine two constants a and b in the model equation (Eq. 3). The solid curve is the model prediction $\Delta h/h$ (Eq. 4) from the solution of Eq. 3.

Another possible binding site is the interior of the hydrocarbon chain region, into which a curcumin molecule may insert and stay bound. We assume that this is the higher energy state (the *I* state) for curcumin. We assume that the *I* state will cause a membrane area expansion, A_I, per molecule but will not cause membrane thinning. Then the membrane thinning by curcumin binding is given by Eq. 1.

To express $N(S)/L$ in terms of the curcumin/lipid ratio C_b/L, we need to know the energy difference between the *S* state and the *I* state; and we believe that the crucial idea is that the elastic energy of membrane thinning must be included in the energy level of the S state. This energy can be derived as follows (26): A fractional area expansion $\Delta A/A$ is a strain whose corresponding stress is the monolayer tension $\sigma = (K_a/2)\Delta A/A$, where K_a is the bilayer stretch coefficient (12). The binding of $\delta N(S)$ curcumin molecules causes a change in the energy $\delta E = -\varepsilon_S^o \delta N(S) + \sigma A_S \delta N(S)$, where the first term is the intrinsic binding energy, $-\varepsilon_S^o$, presumably due to hydrophobic interaction, and the second term is the elasticity energy of area stretching (or membrane thinning). Combining this relation with Eq. 1, we obtain the energy level for the *S* state (26):

$$E_S = -\varepsilon_S^o + (K_a/2)(A_S^2/A_L)N(S)/L. \tag{2}$$

The simplest choice for the energy level of the *I* state is a constant $E_I = -\varepsilon_I^o$. Then the ratio of the numbers of curcumin molecules in the *S* state and in the *I* state is $N(S)/N(I) = \exp[-\beta(E_S - E_I)]$, with $\beta^{-1} = k_B T$, the Boltzmann constant times the temperature. From this we obtain the equation for the ratio of curcumin molecules in the *S* state to all curcumin molecules associated with the membrane, $\alpha \equiv N(S)/C_b$ or for $x \equiv \alpha(C_b/L)$:

$$\alpha = \frac{1}{2}\left[1 - \tan h\left(b\frac{C_b}{L}\alpha - a\right)\right] \quad \text{or}$$

$$\frac{x}{C_b/L} = \frac{1}{2}[1 - \tan h(bx - a)], \tag{3}$$

where we have introduced $C_b = N(S) + N(I)$, $a = \beta(\varepsilon_S^o - \varepsilon_I^o)/2$ and $b = \beta K_a(A_S^2/A_L)/4$. Note that the only unknown in b is A_S. $K_a \cong 243$ mN/m has been measured (12). $A_L = 73.4$ Å^2 is calculated from the h of pure DOPC (26.8 Å obtained from $PtP = 36.8$ Å (9)) and its chain volume per lipid (984 Å^3) (27).

The membrane thinning data $\Delta h/h$ vs. C_b/L is interpreted as x vs. C_b/L by rewriting Eq. 1 as

$$-\Delta h/h = (A_S/A_L)(C_b/L)\alpha = (A_S/A_L)x. \tag{4}$$

Thus we can directly compare the solution of our model, Eq. 3, with the data. We first select two points in the data to determine the two unknown constants a and b. We assume

that the initial binding is to the S state, i.e., $\alpha \to 1$ as $C_b/L \to 0$. So the initial slope of $\Delta h/h$ vs. C_b/L equals A_S/A_L (this required a continuous curve fitting to the data). This gives $A_S = 330\,\text{Å}^2$, and $b = 218$. Next we find the point of intersection between the line $x = (1/2)C_b/L$ and the data curve x vs. C_b/L. At this point of intersection, called $x_{1/2}$, the relation $bx_{1/2} = a$ is satisfied (see Eq. 3). From the value of intersection $x_{1/2} \sim 0.005$ and the value of b, we obtained $a = 1.1$.

With a and b determined, we then solved Eq. 3 for α or x and used Eq. 4. to reproduce $\Delta h/h$ as a function of C_b/L. The solution is compared with the data in Fig. 4; the agreement of the model with the data is excellent.

We note that if we were to assume that E_S is a constant, not including the elastic energy of membrane thinning, then α would be a constant and x would be proportional to C_b/L. Then by Eq. 4, $\Delta h/h$ vs. C_b/L would be a straight line, strongly disagreeing with the data.

Membrane area expansion

Our model also predicts what to expect from the membrane area expansion experiment. Since the initial membrane thinning was due to curcumin initially bound mostly to the S state, the area expansion should be $\Delta A/A \sim -\Delta h/h$ for the low C_b/L region. As the binding to the I state increased, the area expansion $\Delta A/A$ should become larger than $-\Delta h/h$. This is because in our model we assume that curcumin in the I state would cause area expansion but no thickness change.

In each of our GUV experiments, the vesicle projection inside the micropipette was observed to reach an equilibrium length. From this equilibrium length, we calculated the final fractional area expansion $\Delta A/A$ as a function of curcumin concentration in solution. To compare with the membrane thinning measurement, we will need to know the amount of curcumin bound to the GUV at each curcumin concentration. This was achieved by using the partition coefficient from solution to lipid bilayers measured previously by isothermal titration calorimetry (9): $C_b/L = KC_f$, $K = 2.4 \times 10^4\ \text{M}^{-1}$, where C_f is the curcumin concentration in solution. In Fig. 5, $\Delta A/A$ was plotted as a function of C_b/L for the upper and lower limit measurements. The bottom curve shows the equivalent fractional area expansion $(\Delta A/A)_{\Delta h/h} = -\Delta h/h$ from the fractional thinning data shown in Fig. 4. Since $(\Delta A/A)_{\Delta h/h}$ does not include the area expansion due to the curcumin in the I state, it is smaller than the total area expansion that falls somewhere between the upper and lower limits.

Note that the curcumin/lipid ratios C_b/L of the x-ray data (the bottom curve of Fig. 5) were accurate because the curcumin concentrations in the experimental samples for x-ray diffraction were directly measured spectroscopically (9). In contrast, the C_b/L for the GUV experiment had an uncertainty of approximately $\pm 10\%$ (due to curcumin's tendency to adsorb to the containers' walls; see Sample preparation). This uncertainty in concentration made the GUV experiment unsuitable in low C_b/L regions (<0.03) (due to the very large slope in $\Delta A/A$ vs. C_b/L). Nevertheless, the GUV results presented in Fig. 5 unambiguously confirmed the two-state model described in the last section.

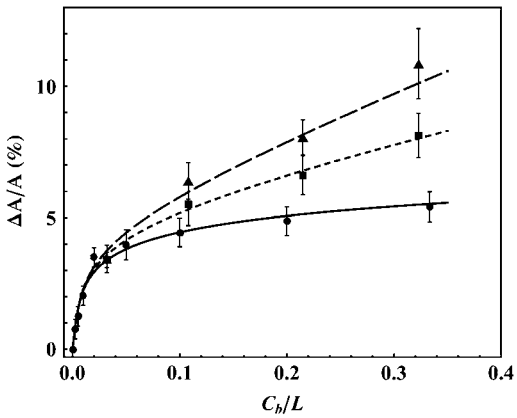

FIGURE 5 Fractional area expansion measured by GUV experiments (*squares* and *triangles*) compared with the values corresponding to the membrane-thinning measurement by x-ray (*solid circles*). The square and triangle data are the asymptotic values $\Delta A/A$ taken from the lower and upper limit measurements in Fig. 3, respectively; the error bars represent the standard deviations. The real area expansion effect of curcumin falls between the upper and lower limits. The curves are the results from the model as explained in the text.

The fractional area expansion by the two-state model is given by

$$\begin{aligned}\Delta A/A &= (A_S/A_L)(C_b/L)\alpha + (A_I/A_L)(C_b/L)(1-\alpha)\\ &= (\Delta A/A)_{\Delta h/h} + (A_I/A_L)(C_b/L)(1-\alpha). \qquad (5)\end{aligned}$$

Since α is already determined by Eq. 3, the model allows only one undetermined parameter A_I for the GUV results. In Fig. 5, we used Eq. 5 and different values of A_I (12 Å^2 and 6 Å^2, respectively) to fit the upper and lower limits of the curcumin effect (the top two *curves*). The real effect is in between these two limits. It is clear that the measured membrane area expansion by curcumin binding is consistent with the two-state model. Eq. 5 predicted that at small values of C_b/L where α is close to 1 (e.g., $C_b/L = 0.032$), the fractional area expansion of GUV should be close to the value of $(\Delta A/A)_{\Delta h/h}$, and at larger values of C_b/L (>0.032) where α is significantly smaller than 1, the fractional area expansion of GUV should be larger than the value of $(\Delta A/A)_{\Delta h/h}$. Both features were born out by the GUV experiment. The agreement also strongly supports the proposed sites for the two states, one on the interface and another inserted in the hydrocarbon region. The interfacial binding both thins the membrane and expands the area, whereas the insertion among the chains expands the area but has little thinning effect.

The monolayer area expansion per curcumin is $A_S \sim 330$ Å^2 for the S state, and A_I is between 6 Å^2 and 12 Å^2 for the I state. These values are not to be interpreted as the physical dimensions of the curcumin molecule. (The largest and smallest cross sections of curcumin molecular crystal are roughly 122 Å^2 and 22 Å^2, respectively; 28.) A lipid bilayer

is not an inert matrix to which a molecule binds. Rather it is a complex assembly of flexible lipid molecules and water molecules. When a molecule binds to the lipid bilayer, the molecule might bring in additional water molecules or release some water molecules associated with the bilayer before binding. Such a redistribution of water molecules would affect the value of area expansion by molecular binding. For example, the helical lengthwise cross section of melittin is $\sim$400 Å^2, but the measured A_S for melittin is only 175–246 Å^2, depending on the lipid compositions (26).

CONCLUSION

Curcumin binding to lipid bilayers follows the same binding pattern of amphipathic peptides (26). Both curcumin and peptides initially bind to the interface and then at higher concentrations gradually partition to a state inserted into the hydrocarbon region. The main difference is that curcumin binds in both states as monomers (Eq. 3 is valid only for monomers). On the other hand, amphipathic peptides bind to the interface as monomers but insert into the hydrocarbon region to form pores, each composed of multiple peptides (29). Although curcumin and antimicrobial peptides are both amphipathic molecules, curcumin is far more hydrophobic than the peptides (for example, magainin, 23 amino acids, carries +5 charges). Yet their binding behaviors to lipid bilayers are basically the same. This suggests that the two-state binding of curcumin to lipid bilayers is typical of amphipathic drugs.

The combination of the x-ray experiment for membrane thickness and the GUV experiment for membrane area allows us to determine the numerical values for the relative binding energy $\varepsilon_S^o - \varepsilon_I^o$ and area expansions per molecule A_S and A_I. These values are important for quantitative understanding of interactions with membranes, such as molecular dynamics simulations. Also, the validity of both experimental results is reinforced by mutual agreement.

Drug binding alters the physical properties of the lipid bilayer, including a decrease of the hydrocarbon thickness and softening of its elastic rigidity (2,9). Functions of some membrane proteins have been shown to depend on such physical properties of their host lipid bilayers, for example, mechanosensitive channels (30) and gramicidin channels (2). The result reported here suggests the possibility that drugs influence functions of membrane proteins via their interactions with lipid bilayers.

This work was supported by National Institutes of Health grant GM55203 and the Robert A. Welch Foundation grant C-0991 to (H.W.H.) and by National Science Council (Taiwan) contracts NSC 95-2112-M-145-001 (to W.-C.H.), NSC 95-2112-M-008-018-MY3 to (F.-Y.C.), and NSC 96-2112-M-213-007-MY3 to (M.-T.L.).

REFERENCES

1. Sheetz, M. P., and S. J. Singer. 1974. Biological membranes as bilayer couples. A molecular mechanism of drug-erythrocyte interactions. *Proc. Natl. Acad. Sci. USA.* 71:4457–4461.
2. Ingolfsson, H. I., R. E. Koeppe 2nd, and O. S. Andersen. 2007. Curcumin is a modulator of bilayer material properties. *Biochemistry.* 46:10384–10391.
3. Wiggins, P., and R. Phillips. 2004. Analytic models for mechanotransduction: gating a mechanosensitive channel. *Proc. Natl. Acad. Sci. USA.* 101:4071–4076.
4. Jaruga, E., A. Sokal, S. Chrul, and G. Bartosz. 1998. Apoptosis-independent alterations in membrane dynamics induced by curcumin. *Exp. Cell Res.* 245:303–312.
5. Khajavi, M., K. Shiga, W. Wiszniewski, F. He, C. A. Shaw, J. Yan, T. G. Wensel, G. J. Snipes, and J. R. Lupski. 2007. Oral curcumin mitigates the clinical and neuropathologic phenotype of the Trembler-J mouse: a potential therapy for inherited neuropathy. *Am. J. Hum. Genet.* 81:438–453.
6. Joe, B., M. Vijaykumar, and B. R. Lokesh. 2004. Biological properties of curcumin-cellular and molecular mechanisms of action. *Crit. Rev. Food Sci. Nutr.* 44:97–111.
7. Maheshwari, R. K., A. K. Singh, J. Gaddipati, and R. C. Srimal. 2005. Multiple biological activities of curcumin: a short review. *Life Sci.* 78:2081–2087.
8. Mall, M., and K. Kunzelmann. 2005. Correction of the CF defect by curcumin: hypes and disappointments. *Bioessays.* 27:9–13.
9. Hung, W. C., F. Y. Chen, C. C. Lee, Y. Sun, M. T. Lee, and H. W. Huang. 2008. Membrane thinning effect of curcumin. *Biophys. J.* 94:4331–4338.
10. Oetari, S., M. Sudibyo, J. N. Commandeur, R. Samhoedi, and N. P. Vermeulen. 1996. Effects of curcumin on cytochrome P450 and glutathione S-transferase activities in rat liver. *Biochem. Pharmacol.* 51:39–45.
11. Longo, M. L., A. J. Waring, L. M. Gordon, and D. A. Hammer. 1998. Area expansion and permeation of phospholipid membrane bilayer by influenza fusion peptides and melittin. *Langmuir.* 14:2385–2395.
12. Rawicz, W., K. C. Olbrich, T. McIntosh, D. Needham, and E. Evans. 2000. Effect of chain length and unsaturation on elasticity of lipid bilayers. *Biophys. J.* 79:328–339.
13. Tennesen, H. H. 2002. Solubility, chemical and photochemical stability of curcumin in surfactant solutions. Studies of curcumin and curcuminoids, XXVIII. *Pharmazie.* 57:820–824.
14. Angelova, M. I. 2000. Liposome electroformation. *In* Giant Vesicles. P. L. Luisi and P. Walde, editors. John Wiley & Sons, Chichester, UK. 27–36.
15. Kwok, R., and E. Evans. 1981. Thermoelasticity of large lecithin bilayer vesicles. *Biophys. J.* 35:637–652.
16. Zhelev, D. V., and D. Needham. 1993. Tension-stabilized pores in giant vesicles: determination of pore size and pore line tension. *Biochim. Biophys. Acta.* 1147:89–104.
17. Fygenson, D. K., M. Elbaum, B. Shraiman, and A. Libchaber. 1997. Microtubules and vesicles under controlled tension. *Phys. Rev. E Stat. Phys. Plasmas Fluids Relat. Interdiscip. Topics.* 55:850–859.
18. Hwang, T. C., R. E. Koeppe 2nd, and O. S. Andersen. 2003. Genistein can modulate channel function by a phosphorylation-independent mechanism: importance of hydrophobic mismatch and bilayer mechanics. *Biochemistry.* 42:13646–13658.
19. Seemann, H., and R. Winter. 2003. Volumetric properties, compressibilities, and volume fluctuations in phospholipid-cholesterol bilayers. *Z. Phys. Chem.* 217:831–846.
20. Zasloff, M. 2002. Antimicrobial peptides of multicellular organisms. *Nature.* 415:389–395.
21. Banerjee, U., R. Zidovetzki, R. R. Birge, and S. I. Chan. 1985. Interaction of alamethicin with lecithin bilayers: a 31P and 2H NMR study. *Biochemistry.* 24:7621–7627.
22. Heller, W. T., A. J. Waring, R. I. Lehrer, and H. W. Huang. 1998. Multiple states of beta-sheet peptide protegrin in lipid bilayers. *Biochemistry.* 37:17331–17338.
23. Huang, H. W., and Y. Wu. 1991. Lipid-alamethicin interactions influence alamethicin orientation. *Biophys. J.* 60:1079–1087.
24. Ludtke, S. J., K. He, Y. Wu, and H. W. Huang. 1994. Cooperative membrane insertion of magainin correlated with its cytolytic activity. *Biochim. Biophys. Acta.* 1190:181–184.

25. Israelachvili, J. 1991. Intermolecular & Surface Forces. Academic Press, London.

26. Lee, M. T., F. Y. Chen, and H. W. Huang. 2004. Energetics of pore formation induced by membrane active peptides. *Biochemistry*. 43: 3590–3599.

27. Armen, R. S., O. D. Uitto, and S. E. Feller. 1998. Phospholipid component volumes: determination and application to bilayer structure calculations. *Biophys. J*. 75:734–744.

28. Tonnesen, H. H., J. Karlsen, and A. Mostad. 1982. Structural studies of curcuminoids. I. The crystal structure of curcumin. *Acta Chem. Scand. B*. 36:475–479.

29. Huang, H. W. 2000. Action of antimicrobial peptides: two-state model. *Biochemistry*. 39:8347–8352.

30. Sukharev, S., M. Betanzos, C. S. Chiang, and H. R. Guy. 2001. The gating mechanism of the large mechanosensitive channel MscL. *Nature*. 409:720–724.